2024, 21(9): 2970-2983
https://doi.org/10.21123/bsj.2024.9306
P-ISSN: 2078-8665 - E-ISSN: 2411-7986
Baghdad Science Journal

Limit Cycles of the Three-dimensional Quadratic Differential System via Hopf Bifurcation

Aram A. Abddulkareem[*1]**, *Azad I. Amen***[2,3,4]**, *Niazy H. Hussein***[5,6]

[1]Department of Mathematics, Faculty of Education, Soran University, Soran, Iraq.
[2]Department of Mathematics, College of Basic Education, Salahaddin University-Erbil, Erbil, Iraq.
[3]Department of Mathematics, Basic Education College, Raparin University, Ranya, Iraq.
[4]Department of Mathematics, College of Science, Duhok University, Duhok, Iraq.
[5]Department of Mathematics, Faculty of Science, Soran University, Soran, Iraq.
[6]Department of Mathematics, College of Education, Salahaddin University-Erbil, Erbil, Iraq.
*Corresponding Author.

Received 09/09/2023, Revised 18/12/2023, Accepted 20/12/2023, Published Online First 20/02/2024, Published 01/09/2024

Abstract

In this study, the quadratic 3-dimensional differential system is considered, in which the origin of the coordinate becomes the Hopf equilibrium point. The existence and stability of limit cycles that emerge from the Hopf point are being investigated. The Lyapunov coefficients connected to the Hopf point are calculated using the projection method. First, four families of parameter conditions are driven by which the quadratic 3-dimensional differential system can exhibit codimension three of the Hopf bifurcation. The analytical proof of each parameter family of conditions is given by calculating the Lyapunov coefficients, the vanishing of the first, sconed Lyapunov, and the non-zero of the third Lyapunov coefficients. The explicit conditions are presented for the existence and stability of three limit cycles arising from each family of Hopf bifurcations. The output of existence displays a stable (unstable) Hopf point, accompanied by the emergence of two stable (unstable) limit cycles alongside one unstable (stable) limit cycle in the neighborhood of the unstable (stable) origin of the coordinated 3-dimensional quadratic system. In addition, the outcome is utilized for exploring the limit cycles of the n-scroll chaotic attractor system, which has many practical uses, including secure communication, encryption, random number generation, and autonomous mobile robots. The conditions are derived under which the origin point of this system becomes the Hopf point, and three limit cycles can exist around the Hopf point. Finally, the numerical demonstrations show that the system undergoes a supercritical Hopf bifurcation, resulting in two stable and one unstable limit cycle. Furthermore, all results are verified.

Keywords: Hopf bifurcation, Limit cycles, Lyapunov coefficient, n-scroll chaotic attractors, Quadratic 3-dimensional differential systems.

Introduction

The number of limit cycles that a particular differential system can have is one of the significant challenges in the qualitative theory of differential systems. The number of limit cycles in R^2 is finite [1-3]. For R^n, $n \geq 3$, the situations are vastly different. Determining the number of limit cycles in the

2024, 21(9): 2970-2983
https://doi.org/10.21123/bsj.2024.9306
P-ISSN: 2078-8665 - E-ISSN: 2411-7986
Baghdad Science Journal

quadratic 3-dimensional differential system is challenging. Some quadratic vector fields in R^3 have an unlimited number of limit cycles[4]. The dynamic richness of quadratic 3-dimensional differential systems makes them incredibly valuable in various fields, including cryptography, image encryption, non-linear control systems, signal processing, and time series prediction. The Liu system, the Lorenz system, the Rossler system, the Chen system, and the Rikitake system are all examples of quadratic systems in R^3.

The analytical solution to the quadratic 3-dimensional differential system is elusive[5]. However, several alternative approaches and areas of study can be explored: numerical methods[6], computer simulations[7], and qualitative analysis. It can gain insights into the system's behavior through qualitative analysis. The study involves analyzing the qualitative properties of solutions, such as equilibrium point stability and limit cycle existence.

For this purpose, that is, the search for analytical results that give information about the existence and location of limit cycles, this quadratic three-dimensional first-order differential system will be studied.

$$\begin{aligned}\dot{x}(t) &= \lambda x(t) - \mu y(t) + a_1 x^2(t) + a_2 x(t)y(t) + a_3 x(t)z(t) + a_4 y^2(t) + a_5 y(t)z(t) + a_6 z^2(t),\\ \dot{y}(t) &= \mu x(t) + \lambda y(t) + b_4\left(y^2(t) - x^2(t)\right) + b_2 x(t)y(t) + b_3 x(t)z(t) + b_5 y(t)z(t) + b_6 z^2(t), \\ \dot{z}(t) &= \alpha z(t) + c_1 x^2(t) + c_2 x(t)y(t) + c_3 x(t)z(t) + c_4 y^2(t) + c_5 y(t)z(t) + c_6 z^2(t),\end{aligned} \quad 1$$

where a_i, b_i, c_i, for $i = 1 \dots 6$, λ, α and $\mu > 0$ are real parameters, and $x(t), y(t), z(t)$ are state variables, for simplicity it written in x, y, and z.

Various methodologies, including the classical projection method, computation of singular point quantities, and averaging methods, investigate limit cycles emanating from Hopf points. Some researchers have undertaken analytical studies of quadratic differential systems. They use the projection method to calculate Lyapunov coefficients related to Hopf points, focusing on specific systems with two or three limit cycles and analyzing their stability[8,9]. Others have explored limit cycles via singular quantities (focal values), providing a method to identify more limit cycles without addressing their stability[10]. The Averaging method represents another approach to analytically studying limit cycles, although it presents challenges in calculating high zeros in equations[11]. In contrast, some researchers opt for a numerical exploration of limit cycles, leveraging this strategy to uncover more limit cycles[11,12].

In this note, the projection method is used to study and analyze the limit cycles related to the Hopf point. This method allowed us to calculate the first three Lyapunov coefficients, and in the neighborhood of Hopf point, granted the existence of three limit cycles. Our result deals with general differential systems of degree 2, which in this form were not considered before. The four families of parameter conditions drive the existence of three limit cycles. Our system and conditions differ from particular systems in previous studies[8-12]. Moreover, the stability of limit cycles is investigated. All results in this study were verified and numerically studied by the Maplesoft program.

The present research is structured in the following manner. The concept of Hopf bifurcation is elucidated by using the projection technique. The definition and Lyapunov coefficients have been given in this paper. The main result of our investigation has been documented and verified. In the subsequent part, The quadratic differential system that encompasses n-scroll chaotic attractors is examined, serving as an illustrative illustration of the main outcome. The main result of our study was used to make estimations concerning the presence and stability of the three limit cycles associated with the origin Hopf point. The numerical simulations are carried out using precise parameter values to validate and demonstrate the analytical findings.

2024, 21(9): 2970-2983
https://doi.org/10.21123/bsj.2024.9306
P-ISSN: 2078-8665 - E-ISSN: 2411-7986
Baghdad Science Journal

Materials and Methods

Review on Hopf bifurcation

This section provides a comprehensive overview of the projection method[13]. This method is used to compute the first and second Lyapunov coefficients related to Hopf bifurcations. This method was additionally employed to compute the third and fourth Lyapunov coefficients[14].

Consider the following general differential equation,

$$\dot{X} = f(X, \delta). \qquad 2$$

Suppose that f is a class of $C^{\infty} \in R^3 \times R^n$, where vector $X \in R^3$ denotes phase variables and the vector $\delta \in R^n$ represents control parameters. Suppose $X = X_0$ is an equilibrium point of system 2 at $\delta = \delta_0$. Moving the equilibrium X_0 to the origin of the coordinates by the linear change of the variable $X - X_0$. Also, by X, it expresses

$$F(X) = f(X, \delta_0), \qquad 3$$

as

$$F(X) = AX + \frac{1}{2}B(X,X) + \frac{1}{6}C(X,X,X) + \frac{1}{24}D(X,X,X,X) + \cdots,$$

where $A = f_X(0, \delta_0)$ and for $i = 1, 2, 3$,

$$B_i(X,Y) = \sum_{j,k=1}^{3} \frac{\partial^2 F_i(\xi)}{\partial \xi_j \partial \xi_k}|_{\xi=0} X_j Y_k, \qquad C_i(X,Y,Z) = \sum_{j,k,l=1}^{3} \frac{\partial^3 F_i(\xi)}{\partial \xi_j \partial \xi_k \partial \xi_l}|_{\xi=0} X_j Y_k Z_l,$$

are two multilinear functions. Suppose that at equilibrium $(0, \delta_0)$, A has an eigenvalue $\lambda_1 \neq 0$ with a pair of complex eigenvalues on the imaginary axis: $\lambda_{2,3} = \pm i\omega_0$, $(\omega_0 > 0)$, and the eigenvalues $\lambda_{2,3}$ are the only eigenvalues with $Re(\lambda) = 0$. Assuming that T^c is the generalized eigenspace of A that relates to $\lambda_{2,3}$. Let p, and q be vectors in C^3 in a way that

$$Aq = i\omega_0 q, \quad A^T p = -i\omega_0 p, \quad \langle p, q \rangle = 1, \qquad 4$$

where A^T is the transposed of the matrix A. Any vector $y \in T^c$ could be stated as $y = wq + \bar{w}\bar{q}$, in which $w = \langle p, y \rangle \in C$ and $\bar{w}$ is the conjugate of w. By using an immersion of the form $X = H(w, \bar{w})$, it is possible to parameterize the 2-dimensional center manifold related to the eigenvalues $\lambda_{2,3}$ by w and $\bar{w}$, where $H: C \to R^3$ has a Taylor series of the form

$$H(w,\bar{w}) = wq + \bar{w}\bar{q} + \sum_{2 \le j+k \le 7} \frac{1}{j!\,k!} h_{jk} w^j \bar{w}^k + O(|w|^8),$$

with $h_{jk} \in C^3$ and $h_{jk} = \bar{h}_{kj}$. Substituting the above expression into Eq. 2, the following differential equation was obtained

$$H_w w' + H_{\bar{w}} \bar{w}' = F\big(H(w,\bar{w})\big), \qquad 5$$

in which F is expressed by Eq. 3. By solving the system of linear equations described by the coefficients in Eq. 5, the complex vectors h_{ij} are produced, taking the coefficients F into consideration, so that Eq. 5, on the chart w for a central manifold, writes as follows:

$$w = i\omega_0 w + \tfrac{1}{2} G_{21} w\,|w|^2 + \tfrac{1}{12} G_{32} w\,|w|^4 + \tfrac{1}{144} G_{43} w\,|w|^6 + O(|w|^8), \qquad 6$$

with $G_{(i+1)i} \in C$. The first, second, and third Lyapunov coefficient l_1, l_2, l_3 can be written as

$$l_1 = \tfrac{1}{2} ReG_{21}, \; l_2 = \tfrac{1}{12} ReG_{32}, \; l_3 = \tfrac{1}{144} ReG_{43}. \qquad 7$$

The explicit expressions for the Lyapunov coefficients can be found in Kuznetsov's book and Sotomayor et al. research[13,14].

A Hopf point of codimension 1 is an equilibrium point (X_0, δ_0) such that the linear part of the vector field f has eigenvalues $\lambda_2 = \lambda$ and $\lambda_3 = \bar{\lambda}$ with $\lambda = \lambda(\delta) = Re(\lambda) + iIm(\lambda)$ $Re(\lambda) = \delta_0 = 0, Im(\lambda) = \omega_0 > 0$, the other eigenvalue $\lambda_1 \neq 0$ and the first Lyapunov coefficient, $l_1(\delta_0)$ is different from zero. A transversal Hopf point is a Hopf point of codimension one for which the complex eigenvalues, depending on the parameters, cross the imaginary axis with a non-zero derivative. In a neighborhood of a transversal Hopf point with $l_1 \neq 0$ the dynamic behavior of the system 2, reduced to the family of

2024, 21(9): 2970-2983
https://doi.org/10.21123/bsj.2024.9306
P-ISSN: 2078-8665 - E-ISSN: 2411-7986
Baghdad Science Journal

parameter-dependent continuations of the center manifold, is orbitally topologically equivalent to the following complex normal form $w' = (\delta_0 + i\omega_0)w + l_1 w|w|^2$, where $w \in C$; δ_0, ω_0, and l_1 are real functions having derivatives of arbitrary higher order. As $l_1 < 0$ ($l_1 > 0$) one family of stable (unstable) limit cycles can be found on the center manifold and its continuation, shrinking to the Hopf point.

A Hopf point of codimension 2 is a Hopf point where l_1 vanishes. It is called transversal if $\delta_0 = 0$ and $l_1 = 0$ have transversal intersections. In a neighborhood of a transversal Hopf point of codimension 2 with $l_2 \neq 0$ the dynamic behavior of the system 2, reduced to the family of parameter-dependent continuations of the center manifold, is orbitally topologically equivalent to $w' = (\delta_0 + i\omega_0)w + \tau_1 w|w|^2 + l_2 w|w|^4$, where δ_0 and τ_1 are unfolding parameters.

A Hopf point of codimension 3 is a Hopf point of codimension 2, where $l_2 = 0$. It is called transversal if $\delta_0 = 0, l_1 = 0$ and $l_2 = 0$ have transversal intersections. In a neighborhood of a transversal Hopf point of codimension 3 with $l_3 \neq 0$ the dynamic behavior of the system 2, reduced to the family of parameter-dependent continuations of the center manifold, is orbitally topologically equivalent to $w' = (\delta_0 + i\omega_0)w + \tau_1 w|w|^2 + \tau_2 w|w|^4 + l_3 w|w|^6$, where δ, τ_1 and τ_2 are unfolding parameters. The bifurcation diagrams for $l_3 \neq 0$ can be found in Takens's research[15]

Main results

First, take into consideration

$$\mathcal{H} = \{(\lambda, \mu, \alpha) \in R^3 : \lambda = \lambda_c = 0, \mu > 0, \alpha < 0\}.$$

System 1 undergoes Hopf bifurcation at the origin $O(0,0,0)$ if the conditions in $\mathcal{H}$ hold. When $\lambda = 0$, the origin of system 1 is a Hopf point with two purely imaginary complex eigenvalues $\pm i\mu$ and non-zero eigenvalue $\alpha < 0$. The classical projection method calculates the Lyapunov coefficients related to the Hopf point. This helps us ensure that, under certain parameter conditions, the system 1 has three limit cycles by examining its third Lyapunov coefficient.

Now, consider the following families of parameters of the system 1:

$$H_1 = \{a_4 = -a_1, c_1 = 0, c_2 = 0, c_4 = 0\},$$

$$H_2 = \left\{ \begin{array}{c} a_1 = \dfrac{b_2}{2}, a_3 = 0, a_4 = -a_1, a_5 = -b_3, a_6 = 0, b_4 = \dfrac{a_2}{2}, b_5 = 0, b_6 = 0, \\ c_1 = 0, c_3 = 0, c_4 = 0, c_5 = 0 \end{array} \right\},$$

$$H_3 = \left\{ \begin{array}{c} a_1 = \dfrac{b_2}{2}, a_2 = 2b_4, a_3 = 0, a_4 = -a_1, a_5 = -b_3, b_3 = 0, b_5 = 0, \\ c_1 = c_4, c_2 = 0, c_3 = b_2, c_5 = 2b_4 \end{array} \right\},$$

$$H_4 = \left\{ \begin{array}{c} a_1 = 0, a_2 = 0, a_3 = 0, a_5 = 0, a_6 = 0, b_1 = 0, b_2 = 2a_4, b_3 = 0, b_4 = 0, b_5 = 0, \\ c_1 = 0, c_3 = a_4, c_4 = 0, c_5 = 0 \end{array} \right\}$$

The following is the main result, which gives the Lyapunov coefficient for system 1:

Theorem 1: Consider system 1 with parameter values in $\mathcal{H}$. Then the origin O is Hopf point. If $\lambda \neq \lambda_c$, then system 1 features a transversal Hopf point at the origin. Moreover,

(a) Consider the conditions in H_1. Then, the first and second Lyapunov vanishes. Moreover, the third Lyapunov coefficient at the origin is given by

$$l_3(H_1) = \frac{H_{11}H_{12}}{3456}\mu^5 . \qquad 8$$

(b) Consider the conditions in H_2. Then, the first and second Lyapunov vanishes. Moreover, the third Lyapunov coefficient at the origin is given by

$$l_3(H_2) = \frac{b_3 c_2^2 \, (a_2^2 + b_2^2) H_{21}}{48\alpha\mu^2(\alpha^2 + 9\mu^2)(\alpha^2 + 4\mu^2)(\alpha^2 + \mu^2)}. \qquad 9$$

(c) Consider the conditions in H_3. Then, the first and second Lyapunov vanishes. Moreover, the third Lyapunov coefficient at the origin is given by

$$l_3(H_3) = \frac{2c_4^3 H_{31}}{\alpha^3\mu(\alpha^2 + \mu^2)} . \qquad 10$$

(d) Consider the conditions in H_4. Then, the first and second Lyapunov vanishes. Moreover, the third Lyapunov coefficient at the origin is given by

$$l_3(H_4) = \frac{b_6 c_2^2 H_{41}}{192\mu^3(\alpha^2 + 9\mu^2)(\alpha^2 + 4\mu^2)^2(\alpha^2 + \mu^2)} \qquad 11$$

If $l_{3(H_i)} \neq 0$ for $i = 1 \dots 4$, then there exist three limit cycles near the equilibrium point at the origin. Where, $H_{11}, H_{12}, H_{21}, H_{31}$, and H_{41} are given below.

$$H_{11} = (4a_1^2 - 4a_1b_2 + a_2^2 - 4a_2b_4 + b_2^2 + 4b_4^2),$$

$$H_{12} = -(4a_1^3a_2 + 16a_1^3b_4 + 12a_1^2b_2b_4 + a_1a_2^3 - 3\, a_1a_2b_2^2 - 12a_1a_2b_4^2 - 16a_1b_4^3 + a_2^3b_2 + 3a_2^2b_2b_4 - a_2b_2^3 - b_2^3b_4 - 4b_2b_4^3),$$

$$H_{21} = (\alpha^4b_3 + 6\mu\alpha^3c_6 - \mu^2\alpha^2b_3 + 18\mu^3\alpha c_6 - 8\mu^4b_3),$$

$$H_{31} = (\alpha(a_4b_6c_6 + a_6b_4c_6) + \mu(a_4a_6c_6 - a_6^2c_4 - b_4b_6c_6 - b_6^2c_4)),$$

$$H_{41} = \Big((2\alpha^6 + 138\alpha^4\mu^2 + 904\alpha^2\mu^4 + 1440\mu^6)a_4^3 + (-21\alpha^3\mu^3 - 69\alpha\mu^5)c_6c_2a_4 + (9\alpha^3\mu^3 + 57\alpha\mu^5)b_6c_2^2\Big).$$

Proof of Theorem 1: For parameters in $\mathcal{H}$, the eigenvalues of the Jacobian matrix of system 1 at the origin are $\alpha < 0$, $\pm\omega_0 i$, where $\omega_0 = \mu > 0$. The eigenvectors q and p defined in Eq 4 are

$$p = (i, 1, 0) \quad , \quad q = \left(\frac{i}{2}, \frac{1}{2}, 0\right).$$

To verify the transversal condition of the Hopf bifurcation. Consider system 1, which is dependent on parameter λ. $\zeta = \zeta(\lambda)$ denotes the real part of the pair of complex eigenvalues at the critical parameter $\lambda = \lambda_c = 0$. Which satisfies

$$\zeta'(\lambda_c) = Re \langle p , \left(\frac{dA}{d\lambda}\right)_{\lambda=\lambda_c} q \rangle = 1 \neq 0,$$

where A denotes the Jacobian matrix of system 1 at the origin. Consequently, the transversal condition for the Hopf point holds. Moreover, each case of Theorem 1 is proved independently.

(a) Consider the parameters in the set H_1, The system's bilinear vector function is computed as follows.

$$B(x, y) = ((2a_1y_1 + a_2y_2 + a_3y_3)x_1 + (a_2y_1 - 2a_1y_2 + a_5y_3)x_2 + (a_3y_1 + a_5y_2 + 2a_6y_3)x_3,$$
$$(-2b_4y_1 + b_2y_2 + b_3y_3)x_1 + (b_2y_1 + 2b_4y_2 + b_5y_3)x_2 + (b_3y_1 + b_5y_2 + 2b_6y_3)x_3,$$
$$c_3y_3x_1 + c_5y_3x_2 + (c_3y_1 + c_5y_2 + 2c_6y_3)x_3).$$

Then, the complex vectors are given by

$$h_{11} = (0, 0, 0),$$

$$h_{20} = \left(\frac{2a_2 + 4ia_1 + ib_2 + 2b_4}{6\mu}, \frac{2b_2 - ia_2 - 4ib_4 + 2a_1}{6\mu}, 0\right),$$

$$h_{21} = \frac{1}{48\mu^2}(8a_1b_4 - 2a_2b_2 + i\,(-4a_1^2 - a_2^2 + b_2^2 + 4\, b_4^2\,), 4a_1^2 + a_2^2 - b_2^2 - 4b_4^2 + i(8a_1b_4 - 2a_2b_2) , \quad 0),$$

$$h_{22} = (0, 0, 0),$$

$$h_{30} = \frac{1}{32\mu^2}(3i(3ia_2 + 2ib_4 - 6a_1 - b_2)\ (ia_2 + 2ib_4 - 2a_1 - b_2), (3ia_2 + 6ib_4 - 6a_1 - 3b_2)(ia_2 + 6ib_4 - 2a_1 - 3b_2), 0),$$

$$h_{31} = \frac{1}{288\mu^3}\Big(\Big(16ia_1^3 + (-60ib_2 + 8a_2 + 56b_4)a_1^2 + (4ia_2^2 + (-88ib_4 - 44b_2)a_2 + 12ib_2^2 + 16ib_4^2 + 16b_4b_2)\, a_1 + 2a_2^3 + (7ib_2 - 30b_4)\, a_2^2 + (8ib_2b_4 + 2b_2^2 + 24b_4^2)a_2 + 7(b_2^2 + 4b_4^2)(b_2i + 2b_4)\Big),\ 56a_1^3 + (-28ia_2 - 16ib_4 +$$

2024, 21(9): 2970-2983
https://doi.org/10.21123/bsj.2024.9306
P-ISSN: 2078-8665 - E-ISSN: 2411-7986

$24b_2)a_1^2 + (14a_2^2 + (-8ib_2 + 16b_4)a_2 + 88ib_2b_4 - 30b_2^2 + 56b_4^2)a_1 - 7ia_2^3 + (-12ib_4 + 2b_2)a_2^2 + (-7ib_2^2 + 60ib_4^2 - 44b_4b_2)a_2 - 4(b_2^2 + 2b_4^2)(2ib_4 - b_2), 0\Big).$

Now, the first and second Lyapounv coefficients vanish. $l_1(H_1) = 0$, $l_2(H_1) = 0$, respectively. With more calculations, it obtained that

$$h_{32} = \frac{1}{2304\mu^4}(-h_{321}, ih_{321}, 0),$$

$$h_{321} = (92a_1^2 - 20a_1b_2 + 23a_2^2 - 20a_2b_4 + 23b_2^2 + 92b_4^2)(2a_2b_2 + 4ia_1^2 + ia_2^2 - ib_2^2 - 8a_1b_4 - 4ib_4^2),$$

$$h_{40} = \frac{1}{180\mu^3}(448ia_1^3 + (468ib_2 + 656a_2 + 944b_4)a_1^2 + (-320ia_2^2 + (-976ib_4 + 484b_2)a_2 + 168ib_2^2 - 656ib_4^2 + 664b_4b_2)a_1 - 52a_2^3 + (-125ib_2 - 252b_4)a_2^2 + (-316ib_2b_4 + 80b_2^2 - 312b_4^2)a_2 + 13ib_2^3 - 164ib_2b_4^2 + 80b_2^2b_4 - 112b_4^3, 112a_1^3 + (-164ia_2 - 656ib_4 + 312b_2)a_1^2 + (-80a_2^2 + (-316ib_2 - 664b_4)a_2 - 976ib_2b_4 + 252b_2^2 - 944b_4^2)a_1 + 13ia_2^3 + (168ib_4 - 80b_2)a_2^2 + (-125ib_2^2 + 468ib_4^2 - 484b_4b_2)a_2 - 320ib_2^2b_4 + 448ib_4^3 + 52b_2^3 - 656b_2b_4^2, 0),$$

$$h_{41} = (h_{411}, h_{412}, 0),$$

$$h_{411} = \frac{1}{1280\mu^4}\Big(624ia_1^4 + (-560ib_2 + 816a_2 + 1920b_4)a_1^3 + (-96\&ia_2^2 + (-1968ib_4 - 1168b_2)a_2 - 320ib_2^2 + 608ib_4^2 - 1072b_4b_2)a_1^2 + (204a_2^3 + (556ib_2 - 912b_4)a_2^2 + (-128ib_2b_4 - 84b_2^2 - 848b_4^2)a_2 + 140ib_2^3 + 592ib_2b_4^2 + 336b_2^2b_4 + 1408b_4^3)a_1 - 63ia_2^4 + (204ib_4 + 56b_2)a_2^3 + (10ib_2^2 + 384ib_4^2 - 140b_4b_2)a_2^2 + (-212ib_2^2b_4 - 816ib_4^3 + 88b_2^3 + 336b_2b_4^2)a_2 + (41ib_2^2 - 132ib_4^2 + 148b_4b_2)(b_2^2 + 4b_4^2)\Big),$$

$$h_{412} = \frac{1}{1280\mu^4}\Big(\Big(528a_1^4 + (-592ia_2 - 1408ib_4 + 816b_2)a_1^3 + (-32a_2^2 + (-336ib_2 - 592b_4)a_2 + 848ib_2b_4 - 384b_2^2 - 608b_4^2)a_1^2 + (-148ia_2^3 + (-336ib_4 + 212b_2)a_2^2 + (140ib_2^2 + 1072ib_4^2 + 128b_4b_2)a_2 + 912ib_2^2b_4 - 1920ib_4^3 - 204b_2^3 + 1968b_2b_4^2)a_1 - 41a_2^4 + (-88ib_2 - 140b_4)a_2^3 + (84ib_2b_4 - 10b_2^2 + \&320b_4^2)a_2^2 + (-56ib_2^3 + 1168ib_2b_4^2 - 556b_2^2b_4 + 560b_4^3)a_2 - (204ib_2b_4 - 63b_2^2 + 156b_4^2)(b_2^2 + 4b_4^2)\Big)\Big),$$

$$h_{42} = (h_{421}, h_{422}, 0),$$

$$h_{421} = \frac{1}{17280\mu^5}\Bigg(1088ia_1^5 + (-9520ib_2 - 2912a_2 - 3360b_4)a_1^4 + (544ia_2^2 + (-19936ib_4 - 3056b_2)a_2 + 3984ib_2^2 - 18560ib_4^2 + 7200b_4b_2)a_1^3 + (-1456a_2^3 + (224ib_2 - 4736b_4)a_2^2 + (17104ib_2b_4 + 1920b_2^2 + 11744b_4^2)a_2 - 1696ib_2^3 + 896ib_2b_4^2 + 4848b_2^2b_4 + 20928b_4^3)a_1^2 + \Bigg(68ia_2^4 + (-4984ib_4 - 764b_2)a_2^3 + (-\&1124ib_2^2 + 3840ib_4^2 + 3368b_4b_2)a_2^2 + (-5368ib_2^2b_4 - 6112ib_4^3 - 2492b_2^3 - 10736b_2b_4^2)a_2 + 536(b_2^2 + 4b_4^2)\left(ib_2^2 - \frac{182i}{67}b_4^2 + \frac{9b_4b_2}{67}\right)\Bigg)a_1 - 182a_2^5 + (651ib_2 - 974b_4)a_2^4 + (36ib_2b_4 + 284b_2^2 + 3720b_4^2)a_2^3 + (438ib_2^3 - 168ib_2b_4^2 - 1184b_2^2b_4 - 5120b_4^3)a_2^2 + 900(b_2^2 + 4b_4^2)\left(ib_2b_4 + \frac{17b_2^2}{450} + \frac{52b_4^2}{225}\right)a_2 + 219\left(ib_2 + \frac{218b_4}{73}\right)(b_2^2 + 4b_4^2)^2\Bigg),$$

$$h_{422} = \frac{1}{17280\mu^5}\Bigg(10464a_1^5 + (-3504ia_2 + 5824ib_4 + 832b_2)a_1^4 + (5232a_2^2 + (-3600ib_2 + 288b_4)a_2 + 6112ib_2b_4 - 5120b_2^2 + 20928b_4^2)a_1^3 + (-1752ia_2^3 + (-688ib_4 + 344b_2)a_2^2 + (168ib_2^2 - 896ib_4^2 - 10736b_4b_2)a_2 - 3840ib_2^2b_4 + 18560ib_4^3 + 3720b_2^3 + 11744b_2b_4^2)a_1^2 + \Bigg(654a_2^4 + (-900ib_2 + 72b_4)a_2^3 + (5368ib_2b_4 - 1184b_2^2 + 4848b_4^2)a_2^2 + (-36ib_2^3 - 17104ib_2b_4^2 + 3368b_2^2b_4 + 7200b_4^3)a_2 + 4984(b_2^2 + 4b_4^2)\left(ib_2b_4 - \frac{487b_2^2}{2492} - \frac{15b_4^2}{89}\right)\Bigg)a_1 - 219ia_2^5 + (-536ib_4 + 34b_2)a_2^4 + (-438ib_2^2 + 1696ib_4^2 - 2492b_4b_2)a_2^3 + (1124ib_2^2b_4 - 3984ib_4^3 + 284b_2^3 + 1920b_2b_4^2)a_2^2 - 651(b_2^2 + 4b_4^2)\left(ib_2^2 - \frac{340i}{93}b_4^2 + \frac{764b_4b_2}{651}\right)a_2 - 68(b_2^2 + 4b_4^2)^2\left(ib_4 + \frac{91b_2}{34}\right)\Bigg),$$

$$h_{33} = (h_{331}, h_{332}, 0),$$

$$h_{331} = \frac{1}{144\mu^5}\Big(2ib_2^5 + (10ia_1 - a_2 - b_4)b_2^4 + (16ib_4^2 + (2ia_2 - 28a_1)b_4 - 32a_1a_2)b_2^3 + \big(-8b_4^3 + (72ia_1 - 36a_2)b_4^2 + (-40ia_1a_2 + 128a_1^2 - 32a_2^2)b_4 - (10ia_1 + a_2)(4a_1^2 + a_2^2)\big)b_2^2 + \Big(32ib_4^4 + (8ia_2 - 112a_1)\&b_4^3 + (160ia_1^2 - 40ia_2^2 + 128a_1a_2)b_4^2 - 72(ia_2 - 2a_1)\left(a_1^2 + \frac{1}{4}a_2^2\right)b_4 - 32i\left(a_1^2 + \frac{1}{4}a_2^2\right)^2\Big)b_2 + 128\Big(-\frac{1}{8}b_4^4 + (ia_1 - a_2)b_4^3 + \frac{5}{4}ia_2b_4^2a_1 + \left(a_1^2 + \frac{1}{4}a_2^2\right)(ia_1 + a_2)b_4 + \frac{1}{8}\left(a_1^2 + \frac{1}{4}a_2^2\right)^2\Big)b_4\Big),$$

$$h_{332} = \frac{1}{144\mu^5}\Big(16a_1^5 + (32ia_2 + 128ib_4 + 128b_2)a_1^4 + (8a_2^2 + (8ib_2 + 112b_4)a_2 + 160ib_2b_4)a_1^3 + \Big(16ia_2^3 + (72ib_4 + 36b_2)a_2^2 + (-40ib_2^2 + 160ib_4^2 - 128b_4b_2)a_2 + 32(b_2^2 + 4b_4^2)(ib_4 - b_2)\Big)a_1^2 + (a_2^4 + (2ib_2 + 28b_4)a_2^3 + (-40ib_2b_4 + 32b_2^2 - 128b_4^2)a_2^2 - 18(b_2^2 + 4b_4^2)(ib_2 + 2b_4)a_2 - (b_2^2 + 4b_4^2)^2)a_1 + 2\Big(ia_2^4 + \left(5ib_4 + \frac{1}{2}b_2\right)a_2^3 + 16b_4a_2^2b_2 - 5\left(ib_4 - \frac{1}{10}b_2\right)(b_2^2 + 4b_4^2)a_2 - i(b_2^2 + 4b_4^2)^2\Big)a_2\Big).$$

The complex number G_{43} is given by

$$G_{43} = \frac{1}{23040\mu^5}\Big(-i(ia_2 - 2ib_4 - 2a_1 + b_2)(ia_2 - 2ib_4 + 2a_1 - b_2)(13816a_1^2b_2^2 + 2320a_2b_4b_2^2 + 2320a_1b_2a_2^2 + 39232a_1b_2b_4^2 + 39232a_2b_4a_1^2 - 9712b_4^4 + 17b_2^4 + 17a_2^4 - 2360b_2^2b_4^2 + 7312a_1b_2^3 + 7312a_2^3b_4 + 19264a_2b_4^3 + 19264a_1^3b_2 - 2360a_1^2a_2^2 - 9712a_1^4 + 11520ia_1^2b_2b_4 - 2880ia_1a_2b_2^2 - 11520ia_1a_2b_4^2 + 2880ia_2^2b_2b_4 + 32352b_4a_2a_1b_2 + 20512b_4^2a_1^2 + 13816b_4^2a_2^2 - 2462a_2^2b_2^2 + 3840ia_1^3a_2 + 15360ia_1^3b_4 + 960ia_1a_2^3 - 15360ia_1b_4^3 + 960ia_2^3b_2 - 960ia_2b_2^3 - 960ib_2^3b_4 - 3840ib_2b_4^3)\Big).$$

According to the above computations and the analysis, the third Lyapunov coefficient $l_3(H_1)$ as follows:

$$l_3(H_1) = \frac{H_{11}H_{12}}{3456\mu^5} = \frac{1}{3456\mu^5}(4a_1^2 - 4a_1b_2 + a_2^2 - 4a_2b_4 + b_2^2 + 4b_4^2)(-4a_1^3a_2 - 16a_1^3b_4 - 12a_1^2b_2b_4 - a_1a_2^3 + 3a_1a_2b_2^2 + 12a_1a_2b_4^2 + 16a_1b_4^3 - a_2^3b_2 - 3a_2^2b_2b_4 + a_2b_2^3 + b_2^3b_4 + 4b_2b_4^3). \qquad 12$$

If $l_3(H_1) \neq 0$, then, at the origin, system 1 possesses a transversal Hopf point with codimension three. The sign of the numerator in Eq. 12 determines the sign of the third Lyapunov coefficient $l_3(H_1)$. Therefore, if $H_{11}H_{12} > 0$ then $l_3(H_1) > 0$, the Hopf point I s unstable (weak repelling focus) at the origin, and for each $\lambda < \lambda_c$, close to λ_c, three limit cycles exist, two unstable and one stable near the origin equilibrium point. If $H_{11}H_{12} < 0$ then $l_3(H_1) < 0$, the Hopf point is stable (weak attractor focus) at the origin, and for each $\lambda > \lambda_c$, close to λ_c, three limit cycles exist, two stable and one unstable, near the origin equilibrium point. Theorem 1 case (a) has been successfully proved.

2024, 21(9): 2970-2983
https://doi.org/10.21123/bsj.2024.9306
P-ISSN: 2078-8665 - E-ISSN: 2411-7986
Baghdad Science Journal

(b) Consider the parameter conditions in the set H_2. The bilinear vector function is computed as follows:

$$B(x,y) = \big((b_2y_1 + a_2y_2)x_1 + (a_2y_1 - b_2y_2 - b_3y_3)x_2 - b_3y_2x_3, (-a_2y_1 + b_2y_2 + b_3y_3)x_1 + (b_2y_1 + a_2y_2)x_2 + b_3y_1x_3, c_2y_2x_1 + c_2y_1x_2 + 2c_6y_3x_3\big).$$

In the same way, as described in case (a), the third Lyapunov coefficient is obtained as follows:

$$l_3(H_2) = \frac{b_3c_2^2(a_2^2 + b_2^2)H_{21}}{48\alpha\mu^2(\alpha^2 + 9\mu^2)(\alpha^2 + 4\mu^2)(\alpha^2 + \mu^2)} = \frac{b_3c_2^2(a_2^2 + b_2^2)(\alpha^4b_3 + 6\mu\alpha^3c_6 - \mu^2\alpha^2b_3 + 18\mu^3\alpha c_6 - 8\mu^4b_3)}{48\alpha\mu^2(\alpha^2 + 9\mu^2)(\alpha^2 + 4\mu^2)(\alpha^2 + \mu^2)}. \quad 13$$

In case $l_3(H_2) \neq 0$, transversality of codimension three of a Hopf point at the origin for system 1 hold. For $c_2 \neq 0$, the sign of the third Lyapunov coefficient Eq. 13, is opposite to the sign of b_3H_{21}. If $b_3H_{21} < 0$ then $l_3(H_2) > 0$. The Hopf point is unstable and for $\lambda < \lambda_c$ close to λ_c, three limit cycles exist: two unstable and one stable near the origin equilibrium point. If $b_3H_{21} > 0$, then $l_3(H_2) < 0$. The Hopf point is stable, and for $\lambda > \lambda_c$ close to λ_c, three limit cycles exist: two stable and one unstable near the origin equilibrium point.

(c) Consider the parameter in the set H_3. The bilinear vector function is written as follows:

$$B(x,y) = (-2(a_4y_1 - b_4y_2)x_1 + 2(b_4y_1 + a_4y_2)x_2 + 2a_6x_3y_3, -2(b_4y_1 + a_4y_2)x_1 - 2(a_4y_1 - b_4y_2)x_2 + 2b_6x_3y_3, -2(-c_4y_1 + a_4y_3)x_1 + 2(c_4y_2 + b_4y_3)x_2 - 2(a_4y_1 - b_4y_2 - c_6y_3)x_3).$$

In the same way, as described in case (a), the third Lyapunov coefficient is given by

$$l_3(H_3) = \frac{2c_4^3H_{31}}{\alpha^3\mu(\alpha^2 + \mu^2)} = \frac{2c_4^3(\alpha(a_4b_6c_6 + a_6b_4c_6) + \mu(a_4a_6c_6 - a_6^2c_4 - b_4b_6c_6 - b_6^2c_4))}{\alpha^3\mu(\alpha^2 + \mu^2)}. \quad 14$$

Since $\alpha < 0$, the opposite of the sign of $c_4\,H_{31}$ determines the sign of the third Lyapunov coefficient, given by Eq. 14. If $c_4H_{31} < 0$, then $l_3(H_3) > 0$. The Hopf point is unstable and for $\lambda < \lambda_c$ close to λ_c, three limit cycles exist: one stable and two unstable near the origin equilibrium point. If $c_4H_{31} > 0$, then $l_3(H_3) < 0$. The Hopf point is stable, and for $\lambda > \lambda_c$ close to λ_c, three limit cycles exist: one unstable and two stable, near the origin equilibrium point.

(d) Consider the parameter conditions in the set H_4. The bilinear vector function is written as follows:

$$B(x,y) = (2a_4x_2y_2, 2(a_4x_1y_2 + a_4x_2y_1 + b_6x_3y_3), c_2(y_2 + a_4y_3)x_1 + c_2x_2y_1 + (a_4y_1 + 2c_6y_3)x_3).$$

In the same way, as described in case (a), the third Lyapunov coefficient obtained as follows:

$$l_3(H_4) = \frac{b_6c_2^2H_{41}}{192\mu^3(\alpha^2 + 9\mu^2)(\alpha^2 + 4\mu^2)^2(\alpha^2 + \mu^2)} = \frac{b_6c_2^2}{192\mu^3(\alpha^2 + 9\mu^2)(\alpha^2 + 4\mu^2)^2(\alpha^2 + \mu^2)}\Big((2\alpha^6 + 138\alpha^4\mu^2 + 904\alpha^2\mu^4 + 1440\mu^6)a_4^3 + (-21\alpha^3\backslash mu^3 - 69\alpha\mu^5)c_6c_2a_4 + (9\alpha^3\mu^3 + 57\alpha\mu^5)b_6c_2^2\Big). \quad 15$$

For $c_2 \neq 0$, the sign of the third Lyapunov coefficient, given by Eq. 15, is determined by the sign of b_6H_{41}. If $b_6H_{41} > 0$, then $l_3(H_4) > 0$. The Hopf point is unstable and for $\lambda < \lambda_c$ close to λ_c, three limit cycles exist: one stable and two unstable near the origin equilibrium point. If $b_6H_{41} < 0$, then

$l_3(H_4) < 0$. The Hopf point is stable, and for $\lambda > \lambda_c$ close to λ_c, there exist three limit cycles: one unstable and two stable, near the origin equilibrium point O. The proof of Theorem 1 is now finished.

Limit Cycles of n-Scroll Chaotic Attractor

This section presents a specific differential system as an example of Theorem 1. This theorem is used to examine and analyze both the Hopf bifurcation and the limit cycle of the system. Additionally, numerical simulations are provided to validate our findings.

The existence of differential systems capable of producing n-scroll chaotic attractors is a significant open topic with a challenging solution[16]. n-scroll chaotic attractors have been extensively studied throughout history[17]. Compared to double-scroll oscillators like Lorenz, they offer richer dynamics and a larger maximum Lyapunov exponent[18,19]. This type of system has many practical uses, such as secure communications[20], encryption[21,22], random number generating[23], autonomous mobile robots[24], and other technical fields.

Now, consider the simplest family of systems with n-scroll chaotic attractor[25]. Which is described as follows:

$$\begin{aligned}\dot{X} &= n_1X + n_2Y + n_3Z + n_9\,YZ,\\ \dot{Y} &= m_1X + m_2Y + m_3Z + m_8XZ + m_9YZ,\\ \dot{Z} &= r_1X + r_2Y + r_3Z + r_7XY + r_8XZ + r_9YZ\,.\end{aligned}$$

It set 14 parameters, and tweaking one resulted in an uncommon three-scroll odd attractor[25]. This system is a subsystem of system 1. Under certain conditions, it has been shown that system 16 undergoes Hopf bifurcation and gives rise to three limit cycles emerging from the Hopf equilibrium point. The following theorem describes the third Lyapunov coefficient associated with a Hopf equilibrium point of the system 16.

Theorem 2: Consider system 16 with a family of conditions

$$K = \left\{\begin{matrix} n_1 = \lambda, n_2 = 0, n_3 = -\dfrac{\mu^2}{r_1}, m_1 = \dfrac{m_3 r_1(\alpha-\lambda)}{\mu^2}, m_2 = \alpha, m_8 = \dfrac{m_3 r_1(m_3 n_9 r_1 + m_9\mu^2)}{\mu^4}, \\ r_2 = 0, r_3 = \lambda, r_7 = 0, r_9 = 0 \end{matrix}\right\},$$

where $\mu = \sqrt{-n_3 r_1} > 0$, $\alpha = m_2 < 0$, and $r_1 \neq 0$. Then, for $\lambda = 0$ the origin is a Hopf equilibrium point. Moreover, the third Lyapunov coefficient is given by

$$l_3 = \frac{m_3 n_9 r_1^2 r_8 (m_3^4 n_9^4 r_1^8 - \mu^{12} r_8^4)}{3456\mu^{20}} \neq 0. \qquad 17$$

Proof of Theorem 2: Consider the conditions in the set K. Use the following linear change of variables,

$$x = X, \qquad y = -\frac{m_3 r_1}{\mu^2}X + Z, \qquad z = \frac{r_1}{\mu}Y.$$

Then, system 16 becomes

$$\begin{aligned}\dot{x} &= \lambda x - \mu\, y + a_2 xy + a_5 yz\\ \dot{y} &= \mu\, x + \lambda\, y + b_2 xy,\\ \dot{z} &= \alpha\, z + c_5 yz,\end{aligned} \qquad 18$$

where coefficients are given by

$$a_2 = -\frac{n_9 m_3 r_1^2}{\mu^3}, \qquad a_5 = \frac{n_9 r_1}{\mu}, \qquad b_2 = r_8, \qquad c_5 = \frac{r_1(m_3 n_9 r_1 + m_9\mu^2)}{\mu^3}.$$

It noted that when $\lambda = 0$, the origin of the coordinate of the system 18 is a Hopf point with eigenvalues α and $\pm i\mu$. Now, if $\alpha = m_2 < 0$, and $\mu = \sqrt{-n_3 r_1}$, where $n_3 r_1 < 0$, then the coefficients of the system 18 satisfy the family of parameter conditions H_1. Thus, by Theorem 1 case (a), the first and second Lyapunov coefficients are vanish. From Eq. 12, the third Lyapunov coefficient is given by Eq. 17.

If $h = \frac{r_8\mu^3}{n_9 r_1^2} \neq 0$, for $r_1 \neq 0$, $m_1 \neq 0$ and $r_1(m_1 m_3) < 0$, then, take into consideration of the following sets

$$S_1 = \{r_8 n_9 > 0, m_3 \in (-h, 0) \cup (h, \infty)\},$$
$$S_2 = \{r_8 n_9 < 0, m_3 \in (-\infty, h) \cup (0, -h)\},$$

$$T_1 = \{r_8 n_9 > 0, m_3 \in (-\infty, -h) \cup (0, h)\},$$
$$T_2 = \{r_8 n_9 < 0, m_3 \in (h, 0) \cup (-h, \infty)\}.$$

When the conditions S_1 or S_2 are satisfied. It follows that, $l_3 > 0$, then the origin is a weak repelling focus for the flow of the system 16 restricted to the attracting center manifold. Consequently, for $\lambda < 0$, three limit cycles exist, one stable and two unstable, for appropriate values of the parameters. On the other hand, when the conditions T_1 or T_2 holds. It follows that, $l_3 < 0$, then the origin is a weak attracting focus for the flow of the system 16 restricted to the attracting center manifold. Consequently, for $\lambda > 0$, three limit cycles exist, one unstable and two stable, near the Hopf equilibrium for appropriate values of the parameters.

Now, Let us use a numerical example to illustrate a system 16. Consider the values of the following parameters

$$n_3 = \frac{1}{2}, n_9 = -1, m_1 = -8, m_2 = -2, m_3 = -2, m_8 = -16, r_1 = -2, r_8 = -4, n_2 = r_2 = r_7 = r_9 = 0,$$

and $n_1 = r_3 = \lambda$. According to Theorem 2, For $\lambda = 0$, the origin of system 16 is the Hopf point with a pair of purely imaginary eigenvalues $\mp i$ and the other $\alpha = -2$. Then, to calculate the third Lyapunov, the following values were obtained

$$p = (i, 1, 0), \qquad q = \left(\frac{i}{2}, \frac{1}{2}, 0\right),$$

$$h_{11} = (0,0,0), \qquad h_{20} = (-2.6667 - 0.66667i, -1.3333 + 1.3333i, 0),$$

$$G_{21} = -\frac{20i}{3}, \qquad l_1 = 0,$$

$$h_{21} = (-1.3333 - i, 1 - 1.3333i, 0), \qquad h_{22} = (0,0,0), \quad h_{30} = (12 - 16.5i, -1.5 - 12i, 0),$$

$$h\_31 = (-4.4444 - 7.7778i, -2.2222 + 15.556i, 0),$$

$$G_{32} = -\frac{1700i}{9}, \qquad l_2 = 0,$$

$$h_{32} = (-51.111 - 38.333i, 38.333 - 51.111i, 0),$$

$$h_{40} = (91.022 + 173.16i, 95.289 + 51.911i, 0),$$

$$h_{41} = (124.8 - 185.4i, -126.6 - 163.2i, 0),$$

$$h\_42 = (206.46i, -88.77 + 700.09i, 0),$$

$$h_{33} = (71.111 + 213.33i, -142.22 - 426.67i, 0),$$

$$G_{43} = -5120 - \frac{764721i}{9}.$$

Then, the third Lyapunov coefficient is $l_3 = -35.556 < 0$. The Hopf point, which is located at the origin, is asymptotically stable and for a suitable $\lambda > 0$ close to $\lambda_c = 0$, three limit cycles exist, two stable and one unstable.

Using the *MatCont*[26] continuing numerical bifurcation program to comprehend system dynamics changes and their influence on parameters. Fig. 1 investigates the exploration of the limit cycle starting from the origin Hopf point of the system 16. It shows the limit cycle regarding the parameter and emphasizes the three limit point cycles for various bifurcation parameter values.

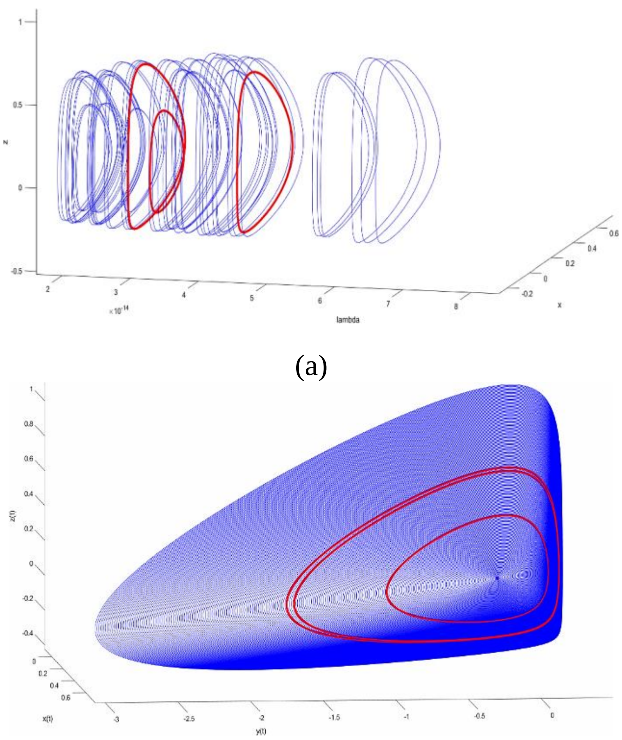

(a)

(b)

Figure 1. The limit point cycles of Hopf bifurcation point for different values of λ of system 16; (a) in $x - y$ plane along line λ, (b) in xyz coordinate plane.

2024, 21(9): 2970-2983
https://doi.org/10.21123/bsj.2024.9306
P-ISSN: 2078-8665 - E-ISSN: 2411-7986
Baghdad Science Journal

Results and Discussion

The present study delves into the dynamics of a quadratic 3-dimensional differential system, focusing on the Hopf equilibrium point at the coordinate origin. Our primary objective is to investigate the existence and stability of limit cycles stemming from this key Hopf point. To achieve this, the classical projection method is employed to calculate the Lyapunov coefficients associated with the Hopf point.

Our investigation uncovers four distinct families of parameter conditions, each leading to a codimension-three Hopf bifurcation in the quadratic 3-dimensional differential system. This exploration is significant for theoretical considerations and has practical implications. Notably, Our findings are leveraged to elucidate the intricacies of the n-scroll chaotic attractor system, a system with broad applications in secure communication and engineering. Precise conditions are established under which the origin point of the n-scroll chaotic attractor system serves as a Hopf point, allowing for the existence of three limit cycles around it. Numerical demonstrations are meticulously conducted to provide empirical support for our theoretical framework, and the robustness of our results is rigorously verified. This comprehensive approach contributes to a deeper understanding of the intricate dynamics within the quadratic 3-dimensional differential system and its practical relevance in real-world applications.

Instead of adding a non-linear perturbation part, studying high-order Lyapunov coefficients for future work is more suitable. Some researchers focus on the numerical calculation of their studied system and may use the projection method to get more results.

Conclusion

In conclusion, our exploration of the quadratic 3-dimensional differential system centered on the Hopf equilibrium point has provided valuable insights into the existence and stability of limit cycles arising from this critical point. Using the classical projection method to compute the Lyapunov coefficients associated with the Hopf point reveals four distinct families of parameter conditions leading to the system's codimension of three Hopf bifurcations. Furthermore, our findings extend to the n-scroll chaotic attractor system, a versatile model with secure communication and engineering applications. The conditions are identified under which the origin point of this system serves as a Hopf point, allowing for three limit cycles around it. The practical implications of these results underscore the significance of our study for real-world applications. The numerical demonstrations validate our theoretical contributions, confirming the robustness and applicability of our derived conditions.

Acknowledgment

The authors acknowledge the referees and the editor for carefully reading this paper and suggesting many helpful comments.

Authors' Declaration

- Conflicts of Interest: None.
- We hereby confirm that all the Figures and Tables in the manuscript are ours. Furthermore, any Figures and images, that are not ours, have been included with the necessary permission for re-publication, which is attached to the manuscript.
- Ethical Clearance: The project was approved by the local ethical committee at University of Soran University.

Authors' Contribution Statement

This work was carried out in collaboration between all authors. A I and N H suggested the idea of the study and supervised the study approach. A A and N H, wrote and edited the manuscript with revised ideas. A A analyzed and calculated the results of the study. All authors read and approved the final manuscript.

References

1. Ilyashenko YS. Finiteness Theorems for Limit Cycles: a Digest of the Revised Proof. Izv Math. 2016 Feb 1; 80(1):50. https://doi.org/10.1070/IM8352
2. Gasull A, Giacomini H. Number of Limit Cycles for Planar Systems with Invariant Algebraic Curves. Qual Theory Dyn Syst. 2023; 22(2): 44. https://doi.org/10.1007/s12346-023-00746-7
3. Llibre J, Rodrıguez G. Configurations of Limit Cycles and Planar Polynomial Vector Fields. J Differ Equ. 2004; 198(2): 374-380. https://doi.org/10.1016/j.jde.2003.10.008
4. Musafirov E, Grin A, Pranevich A, Munteanu F, Şterbeţi C. 3D Quadratic ODE Systems with an Infinite Number of Limit Cycles. In International Conference on Applied Mathematics and Numerical Methods – fourth edition (ICAMNM 2022). ITM Web Conf. 2022; 49: 02006. https://doi.org/10.1051/itmconf/20224902006
5. Llibre J, Martínez YP, Valls C. Limit Cycles Bifurcating of Kolmogorov Systems in R2 and in R3. Commun Nonlinear Sci Numer Simul. 2020; 91: 105401. https://doi.org/10.1016/j.cnsns.2020.105401
6. Sánchez-Sánchez I, Torregrosa J. Hopf Bifurcation in 3-dimensional Polynomial Vector Fields. Commun Nonlinear Sci Numer Simul. 2022;105: 106068. https://doi.org/10.1016/j.cnsns.2021.106068
7. Shiflet AB, Shiflet GW. Introduction to Computational Science: Modeling and Simulation for the Sciences. 2nd edition. USA: Princeton University Press; 2014. 856 p.
8. Dias FS, Mello LF. Non-Linear Differential Systems in the 3–Space: A Note on Periodic Solutions by the Analysis of Two Examples. Math Methods Appl Sci. 2020; 43(7):4383-90. https://doi.org/10.1002/mma.6199
9. Wei Z, Yang Q. Anti-Control of Hopf Bifurcation in the New Chaotic System with Two Stable Node-Foci. Appl Math Comput. 2010; 217(1): 422-429. https://doi.org/10.1016/j.amc.2010.05.035
10. Huang W, Wang Q, Chen A. Hopf Bifurcation and the Centers on Center Manifold for a Class of Three-Dimensional Circuit System. Math Methods Appl Sci. 2020; 43(4): 1988-2000. https://doi.org/10.1002/mma.6026
11. Llibre J, Zhang, X. Hopf Bifurcation in Higher Dimensional Differential Systems via the Averaging Method. Pac J Math. 2009; 240(2): 321-341. https://doi.org/10.2140/pjm.2009.240.321
12. Yu P, Han M. Ten Limit Cycles Around a Center-Type Singular Point in a 3-D Quadratic System with Quadratic Perturbation. Appl Math Lett. 2015; 44: 17-20. http://dx.doi.org/10.1016/j.aml.2014.12.010
13. Yuri A. Kuznetsov. Elements of Applied Bifurcation Theory. 4th edition. Applied Mathematical Sciences (AMS, volume 112). Springer Cham. 19 April 2023; XXVI: 703p. https://doi.org/10.1007/978-3-031-22007-4.
14. Sotomayor J, Mello LF, Braga DD. Bifurcation Analysis of the Watt Governor System. Comput Appl Math. 2007; 26(1): 19-44.
15. Takens F. Unfoldings of Certain Singularities of Vectorfields: Generalized Hopf Bifurcations. J Differ Equ. 1973 Nov 1; 14(3): 476-93. https://doi.org/10.1016/0022-0396(73)90062-4
16. Atiya AN, Hassan HES, Ibrahim KE, ElGhandour OM, Tolba MF. Generalized Formula for Generating N-Scroll Chaotic Attractors. In 2020 2nd Novel Intelligent and Leading Emerging Sciences Conference (NILES), Giza, Egypt. IEEE. 2020 Oct 24; 492-496. https://doi.org/10.1109/NILES50944.2020.9257932
17. Zhang X, Li C. A Novel Type of Chaotic Attractor with a Multiunit Structure: From Multiscroll Attractors to Multi-bond Orbital Attractors. Eur Phys J Plus. 2022 Sep 15; 137(9): 1048. https://doi.org/10.1140/epjp/s13360-022-03268-4
18. Altun K. Multi-Scroll Attractors with Hyperchaotic Behavior Using Fractional-Order Systems. J Circuits Syst Comput. 2022 Mar 30; 31(05): 2250085. https://doi.org/10.1142/S0218126622500852
19. Sugandha K, Singh PP. Generation of a Multi-Scroll Chaotic System via Smooth State Transformation. J Comput Electron. 2022 Aug; 21(4): 781-91. https://doi.org/10.1007/s10825-022-01892-y
20. Tlelo-Cuautle E, Guillén-Fernández O, de Jesus Rangel-Magdaleno J, Melendez-Cano A, Nuñez-Perez JC, de la Fraga LG. Recent Advances in Chaotic Systems and Synchronization: From Theory to Real World Applications. Academic Press; 2019 Jan 1. Chap 15, FPGA implementation of chaotic oscillators, their synchronization, and application to secure communications:301-328. https://doi.org/10.1016/B978-0-12-815838-8.00015-7
21. Al-Bahrani EA, Kadhum RN. A New Cipher Based on Feistel Structure and Chaotic Maps. Baghdad Sci J.

2024, 21(9): 2970-2983
https://doi.org/10.21123/bsj.2024.9306
P-ISSN: 2078-8665 - E-ISSN: 2411-7986
Baghdad Science Journal

2019 Jan 2; 16(1(Suppl.)): 270-80. https://doi.org/10.21123/bsj.2019.16.1(Suppl.).0270
22. Mazher AN, Waleed J. Retina Based Glowworm Swarm Optimization for Random Cryptographic Key Generation. Baghdad Sci J. 2022 Feb 1; 19(1): 0179. https://doi.org/10.21123/bsj.2022.19.1.0179
23. Çiçek S. The Effect of Using Multi-Scroll Chaotic Systems on Chaos-Based Random Number Generators' Performance. J Circuits Syst Comput. 2022 Oct 16; 31(15): 2250259. https://doi.org/10.1142/S0218126622502590
24. Nasr S, Mekki H, Bouallegue K. A Multi-Scroll Chaotic System for a Higher Coverage Path Planning of a Mobile Robot Using Flatness Controller. Chaos, Solitons & Fractals. 2019; 118: 366-75. https://doi.org/10.1016/j.chaos.2018.12.002
25. Elhadj Z, Sprott JC. Simplest 3D Continuous-Time Quadratic Systems as Candidates for Generating Multiscroll Chaotic Attractors. Int J Bifurc Chaos Appl. 2013 Jul; 23(07): 1-6. https://doi.org/10.1142/S0218127413501204
26. Govaerts W, Kuznetsov YA, Meijer HG, Al-Hdaibat B, De Witte V, Dhooge A, et al. Matcount: Continuation Toolbox for ODEs in Matlab. Retrieved December. University of Twente. Netherlands. 2019 Aug; 4: 2020.

دورات النهائية من النظام التفاضلي ثلاثي الأبعاد التربيعية عن طريق تشعب هوبف

ارام عبدالحكيم عبدالكريم[1]، أزاد ابراهيم أمين[4,3,2]، نيازي هادي حسين[6,5]

[1]قسم الرياضيات، الكلية التربية، الجامعة سوران، سوران، اربيل، العراق.
[2]قسم الرياضيات، الكلية التربية الاساس، الجامعة صلاح الدين-اربيل، اربيل، العراق.
[3]قسم الرياضيات، الكلية التربية الاساس، الجامعة رابرين، رانية، العراق.
[4]قسم الرياضيات، الكلية العلوم، الجامعة دهوك، دهوك، العراق.
[5]قسم الرياضيات، الكلية العلوم، الجامعة سوران، سوران، اربيل، العراق.
[6]قسم الرياضيات، الكلية التربية، الجامعة صلاح الدين-اربيل، اربيل، العراق.

الخلاصة

تم في هذه الدراسة النظر في النظام التفاضلي التربيعي ثلاثي الأبعاد، حيث يصبح نقطة الأصل الإحداثيات نقطة توازن هوبف .تم دراسة وجود واستقرار الدورات النهائية التي تنبثق من نقطة هوبف .يتم حساب معاملات ليبانوف المرتبطة بنقطة هوبف باستخدام طريقة الإسقاط .أولاً، تم تحديد أربع عائلات من شروط المعلمات التي من خلالها يمكن للنظام التفاضلي التربيعي ثلاثي الأبعاد أن يظهر البعد الثالث لتشعب هوبف. تم إعطاء الدليل التحليلي لكل مجموعة من الحالات المعلمية عن طريق حساب معاملات ليبانوف، تصفير لقيمة معاملات ليبانوف الأولى و الثاني و غيرالصفري لمعاملات ليبانوف الثالثة. تم تقديم الشروط الواضحة لوجودية واستقرارية ثلاث دورات النهائية ناشئة عن كل عائلة من تشعبات هوبف. يُظهر ناتج الوجود نقطة هوبف مستقرة (غير مستقرة)، مصحوبة بظهور دورتين حديتين مستقرتين (غير مستقرة) جنبًا إلى جنب مع دورة حدية واحدة غير مستقرة (مستقرة) في جوار النقطة الأصل غير المستقر (المستقر) لنظام المعادلة التربيعية ثلاثية الأبعاد. بالإضافة إلى ذلك، يتم استخدام النتيجة لاستكشاف الدورات النهائية لنظام الجذب الفوضوي n-scroll، والذي له العديد من الاستخدامات العملية، بما في ذلك الاتصال الآمن، والتشفير، وتوليد الأرقام العشوائية، والروبوتات المتنقلة المستقلة. تم اشتقاق الشروط التي بموجبها تصبح نقطة الأصل لهذا النظام هي نقطة هوبف، ويمكن أن توجد ثلاث دورات نهائية حول نقطة هوبف .وأخيرًا، توضح العروض العددية أن النظام يخضع لتشعب هوبف فوق الحرج، مما يؤدي إلى دورتين حديتين مستقرتين وواحدة غير مستقرة .وعلاوة على ذلك، تم التحقق من كافة النتائج.

الكلمات المفتاحية: تشعب هوبف، دورات النهائية، معامل ليابونوف، متعدد الممررات لجاذبات الفوضوية، أنظمة تفاضلية تربيعية ثلاثية الأبعاد.